

PICOMETER SCALE EMITTANCE FROM PLASMONIC SPIRAL PHOTOCATHODE FOR PARTICLE ACCELERATOR APPLICATIONS

A. Kachwala*, M. M. Rizi, S. Karkare, Arizona State University, Tempe, AZ, USA

D. Filippetto, Lawrence Berkeley National Laboratory, Berkeley, CA, USA

C. M. Pierce, University of Chicago, Chicago, IL, USA

J. Maxson, Cornell University, Ithaca, NY, USA

Abstract

In this work we demonstrate the generation of a record low root mean square normalized transverse electron emittance of less than 40 pm-rad from a flat metal photocathode – more than an order of magnitude lower than the best emittance that has been achieved from a flat photocathode. This was achieved by using plasmonic focusing of light to a sub-diffraction regime using plasmonic Archimedean spiral structures resulting in a 50 nm root mean square electron emission spot. The emitted electrons show free electron dispersion with ~90% of the total kinetic energy in the transverse direction. Such nanostructured electron sources exhibiting simultaneous spatio-temporal confinement to nanometer and femtosecond levels can be used for developing advanced electron sources to generate unprecedented electron beam brightness for various accelerator applications.

INTRODUCTION

High-repetition rate bunched electron beams have numerous applications in various fields such as research in basic sciences [1], medicine [2] and X-ray generation [3]. Brightness of the electron bunch is a common figure of merit for all these applications. The brightness of the electron bunch is increased by reducing the root mean square normalized transverse emittance of the electron bunch at the photocathode which is expressed in terms of the following [4, 5]:

$$\varepsilon_{n,x} = \sigma_x \sqrt{\frac{\text{MTE}}{m_e c^2}}, \quad (1)$$

where σ_x is the rms electron spot size, MTE is the mean transverse energy of emitted electrons, m_e is the mass of an electron and c is the speed of light.

The emittance at the photocathode can be reduced by either reducing the MTE of the emitted electrons [6, 7] or by reducing the electron emission area from the cathode. The emission area is set by the required bunch charge and the accelerating electric field or by the smallest spot size the laser can be focused to, often limited by the diffraction limit of light. In last few decades, several attempts have been made to reduce the emittance of the electron bunch by reducing the emission area of the photocathode by using nanostructured electron sources [8–10].

In this work we use plasmonic effects driven at a metal dielectric interface to generate electron emission from nano-

scale emission area [11]. The coupling of light and surface plasmon polariton results in highly concentrated optical fields resulting in multi-photon electron emission from a small sub-100 nm scale emission area. Using the plasmonic focusing, we achieve a record low root mean square normalized transverse electron emittance of less than 40 pm-rad from a geometrically flat metal photocathode – more than an order of magnitude lower than the best the emittance that has been achieved from a geometrically flat photocathode [12]. This was achieved by using plasmonic focusing of light to a sub-diffraction regime using plasmonic Archimedean spiral structures resulting in a 50 nm root mean square electron emission spot [13].

Such nanostructured electron sources exhibiting simultaneous spatio-temporal confinement to nanometer and femtosecond level along with a low emittance can be used for developing future ordered electron sources to generate unprecedented electron beam brightness and can revolutionize stroboscopic ultrafast electron diffraction and microscopy as well as next generation miniaturized accelerator applications [14–16].

FINITE DIFFERENCE

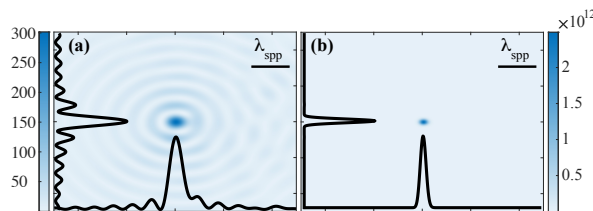


Figure 1: Time averaged (a) surface plasmon polariton intensity (I/I_0) enhancement with $\text{FWHM} \approx 260 \text{ nm}$ and (b) $(I/I_0)^5$ enhancement with $\text{FWHM} \approx 120 \text{ nm}$ at the center of gold Archimedean spiral photocathode obtained with finite difference time domain simulation using circularly polarized Gaussian pulse at 4° angle of incidence, central wavelength of 800 nm and pulse duration of 150 fs as the source of excitation. I is the intensity in the measurement plane and I_0 is the maximum intensity of the incoming excitation pulse and $\lambda_{\text{spp}} = 783 \text{ nm}$.

* akachwal@asu.edu

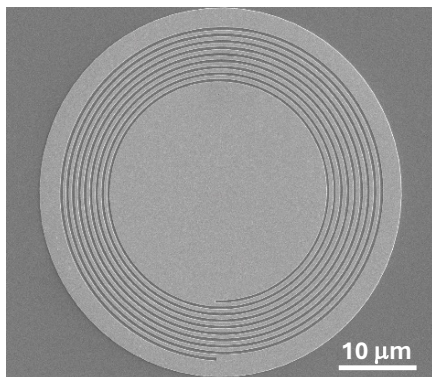


Figure 2: Scanning electron microscope (SEM) image of Archimedean gold spiral on the Si substrate with starting radius (R_0) = 12.5 μm .

TIME DOMAIN SIMULATION

The plasmonic Archimedean spiral photocathode (ASP) was designed using gold for 1.55 eV of photon energy and is known to focus light to few hundred nanometers. To test the focussing performance of the ASP, a finite difference time domain (FDTD) simulation was performed using a commercially available software suite Lumerical [17]. Figure 1(a) shows the intensity enhancement at the center of the spirals with full width at half maximum of ~ 260 nm. According to Fowler-Dubridge theory, the current density for n^{th} order photoemission is directly proportional to I^n , where I is the intensity of the excitation laser [18, 19]. Figure 1(b) shows the electron emission spot size from the center of the spirals considering 5th order photoemission. As we can see, the full width half maximum electron emission spot size is approximately ~ 120 nm or $\sigma_x \sim 50$ nm.

EXPERIMENTAL DETAILS

The simulated geometry was fabricated using electron beam lithography. The details of the fabrication procedure are given elsewhere [20]. Fig. 2 shows the scanning electron microscope (SEM) image of the fabricated spiral.

After a UHV bake-out at 120°C for one day, fabricated ASP was inserted into the PEEM. Initially, it emitted only 0.001 electrons per shot when exposed to a pulsed laser with parameters of 2.5 kW peak power, 150 fs duration, 500 kHz repetition rate, and 800 nm wavelength, focused to 50 μm FWHM at a 4° angle. Within 5 minutes, the emission surged by several orders of magnitude with peak laser power from 0.7 to 2.5 kW. The emission remained stable for days in a 10⁻¹⁰ torr vacuum. Upon removal and re-insertion after the UHV bake, reactivation was necessary, suggesting the ‘laser activation’ process removes adsorbates from the gold emission surface, enhancing photoemission current.

RESULTS AND DISCUSSION

After activation, the spatial distribution of non-linear electron emission spot size was measured as depicted in Fig. 3(a). The root mean square (rms) electron emission spot size was

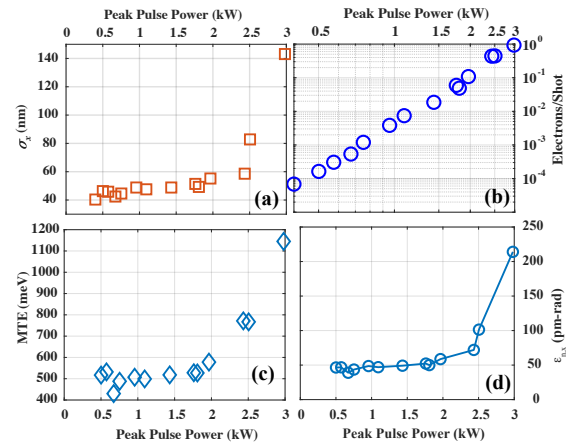


Figure 3: (a) Root mean square electron emission profile measured from the center of the ASP using PEEM over wide range of incident peak pulse power. (b) Logarithmic representation of electrons per shot emitted from ASP as the function of peak laser pulse power. (c) Evolution of experimentally MTE of emitted electrons and (d) Experimentally determined rms normalized transverse emittance at the cathode as a function of peak pulse power of femtosecond laser with the pulse length of 150 fs and central wavelength of 800 nm.

found to be ~ 50 nm, indicating 5th order non-linearity in the photoemission process. This 5th order non-linearity was further supported by measuring the number of electrons per pulse as a function of peak laser pulse power on a double logarithmic scale, as illustrated in Fig. 3(b).

Figure 3 (c) shows evolution of experimentally determined MTE of the emitted electrons as a function of peak laser pulse power. The measurements were performed by operating PEEM in k -space mode with a sub 8 - $\text{m}\text{\AA}^{-1}$ k -space resolution. A detailed description of the measurement procedure can be found elsewhere [23]. The MTE of the emitted electrons is ~ 500 meV over a wide range of peak pulse power. Increase in electron emission spot size and MTE beyond the peak pulse power of ~ 2.5 kW is attributed to Coulomb interaction as seen in Fig. 3(a) and (c).

Next, using Eqn. (1), we calculate the emittance of the electron bunch. This is plotted as a function of peak laser pulse power in Fig. 3(d). Beyond peak pulse power of ~ 2.5 kW, the increase in emittance is attributed to the Coulomb interaction between the emitted electrons. Below ~ 2 kW with less than 0.1 electron/shot the emittance is nearly constant at ~ 50 pm-rad, with the smallest emittance of 40 pm-rad measured at ~ 0.001 electron/shot. These are the smallest emittances achieved from a geometrically flat photocathode. At 0.5–1 electrons/shot, the normalized transverse emittance measured was in the range of 70–200 pm rad respectively.

We plot the 3D distributions of the emitted electrons as a function of the total kinetic energy vs the transverse momentum in the x and y transverse directions. The distributions are cylindrically symmetric in the transverse plane. Fig-

ures 4 a and b show the $k_y = 0$ and $k_x = 0$ cross-sections of this distribution respectively. Electrons are confined within a free electron parabola given by $E = \hbar^2 k_t^2 / 2m_e$ as expected. k_t is the transverse momentum. This parabola is indicated by the dashed white line in Fig. 4. The electrons closer to the central axis of the parabola have a smaller transverse momentum (k_x and k_y) and a larger longitudinal momentum in the direction of emission. For most electron emitters this parabola is uniformly filled in, indicating a uniform distribution in the momentum space [24]. However, Fig. 4 shows a preference for the electrons to be emitted with a preference towards higher transverse momentum states resulting in a parabola that is not uniformly filled in the center.

In the past such a dispersion relation from such plasmonic structures has been attributed to the emission from the Au (111) surface state which follows the dispersion relation of $E = \hbar^2 k_t^2 / 2m^*$, where $m^* = 0.45m_e$ [25]. This dispersion relation is shown by the dashed red lines in Fig. 4. Our results indicate that the electrons are emitted with a dispersion relation closer to the free electron parabola than the parabola with $m^* = 0.45m_e$, indicating that the non-uniform distribution in the transverse momentum space may be due to effects other than emission from the Au (111) surface state.

One explanation of such a behaviour is the interaction of the emitted electron with the plasmonic fields as well as the incident laser pulse. The incident laser pulse excites the plasmons at the metal-dielectric interface, which travel up to approximately 20 μm at a velocity of about $0.93c$. This journey takes ~ 70 fs, shorter than the duration of the 150 fs excitation laser pulse. Consequently, the emitted electrons have the opportunity to interact with both the plasmonic field and the circularly polarized incident laser pulse. These interactions may lead to transfer of momentum between photon/plasmon and the emitted electron [26].

Plasmonic electromagnetic (EM) fields at the center of the ASP exhibit an electric field oscillating in the z -direction and a magnetic field oscillating in the azimuthal (ϕ) direction. Classically, these fields would impart an inward radial momentum to the emitted electrons, qualitatively resulting in dispersion relations resulting in a free electron parabola shown by the white dotted curve in Fig. 4. In addition, inward radial momentum could also result in focusing of the electrons thereby resulting in strong Coulomb interactions at a cross-over very close to the surface for more-than-single-electron-per-shot cases. A comprehensive understanding of the emission mechanism may necessitate a quantum mechanical analysis for precise quantitative explanations. Further investigations are underway to determine the exact cause of such a dispersion and develop a better understanding of photoemission from plasmonic ASP.

CONCLUSION AND FUTURE WORK

In summary, we have developed and analyzed a plasmonics-based electron source that is geometrically flat and exhibits low normalized transverse emittance suitable for UED/M experiments as well as miniaturized particle

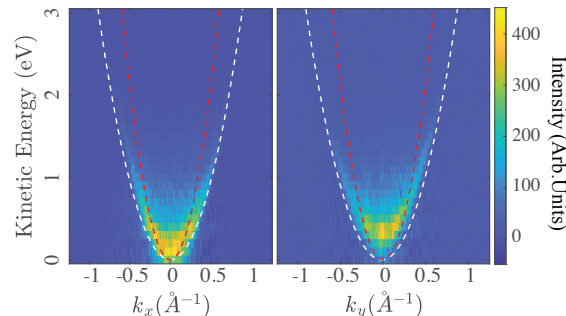


Figure 4: Total kinetic energy vs transverse momentum distributions in k_x and k_y plane of emitted electrons at peak pulse power of ~ 2.4 kW. The distributions are cylindrically symmetric in the transverse plane. The white dotted curve is free electron parabola using the equation $\hbar^2 k_t^2 / 2m_e$. The red dotted curve is plotted using the equation $\hbar^2 k_t^2 / 2m^*$, where $m^* = 0.45m_e$. Here k_t is either k_x or k_y .

accelerators. We attained an unprecedentedly low rms normalized transverse electron emittance of less than 40 pm-rad from a geometrically flat photocathode – a significant improvement compared to the best emittance achieved from geometrically flat cathode. This plasmonics-based electron source, utilizing IR light, holds potential for various applications, including high repetition rate UED/M as well as next-generation particle accelerators.

The dispersion relation correspond to the free energy parabola with $m^* = m_e$. We suspect this dispersion relation arises due to the interaction of the emitted electron with the laser/plasmonic fields leading to momentum transfer in the presence of nanostructured surface non-uniformities at the center of the ASP. Interaction of emitted electron with the plasmonic EM fields could also impart inward radial momentum to the emitted electrons potentially influencing dispersion relations. Further investigations and theoretical modelling are underway to determine the exact cause of such a dispersion and develop a better understanding of photoemission from plasmonic ASP.

ACKNOWLEDGEMENT

This work is supported by the NSF Center for Bright Beams under award PHY-1549132 and Department of Energy Office of Science under awards DE-SC0021092, and DE-SC0021213. C.M.P. acknowledges support from the US DOE SCGSR program. J.M was partially supported by U.S Department of Energy, Grant No. DE-SC0020144.

REFERENCES

- [1] J. Nygard and R. Post. "Recent Advances in High Power Microwave Electron Accelerators for Physics Research." Nuclear Instruments and Methods, vol. 11, Elsevier BV, Jan. 1961, pp. 126–135. doi:10.1016/0029-554x(61)90015-5
- [2] M. Oppelt *et al.* "Comparison Study of in Vivo Dose Response to Laser-Driven versus Conventional Electron Beam." Radiation and Environmental Biophysics, vol. 54, no. 2,

Springer Science and Business Media LLC, 20 Jan. 2015, pp. 155–166. doi: 10.1007/s00411-014-0582-1

[3] B. McNeil and N. Thompson. “X-Ray Free-Electron Lasers.” *Nature Photonics*, vol. 4, no. 12, Springer Science and Business Media LLC, 30 Nov. 2010, pp. 814–821. doi: 10.1038/nphoton.2010.239

[4] D. Dowell and J. Schmerge. “Quantum Efficiency and Thermal Emittance of Metal Photocathodes.” *Physical Review Special Topics - Accelerators and Beams*, vol. 12, no. 7, American Physical Society (APS), 27 July 2009. doi: 10.1103/physrevstab.12.074201

[5] I. Bazarov *et al.* “Maximum Achievable Beam Brightness from Photoinjectors.” *Physical Review Letters*, vol. 102, no. 10, American Physical Society (APS), 11 Mar. 2009. doi: 10.1103/physrevlett.102.104801

[6] P. Saha *et al.* “Physically and Chemically Smooth Cesium-Antimonide Photocathodes on Single Crystal Strontium Titanate Substrates.” *Applied Physics Letters*, vol. 120, no. 19, AIP Publishing, 9 May 2022. doi: 10.1063/5.0088306

[7] A. Kachwala *et al.* “Demonstration of Thermal Limit Mean Transverse Energy from Cesium Antimonide Photocathodes.” *Applied Physics Letters*, vol. 123, no. 4, AIP Publishing, 24 July 2023. doi: 10.1063/5.0159924

[8] E. Simakov *et al.* “Observations of the Femtosecond Laser-Induced Emission From the Diamond Field Emitter Tips.” *Proceedings of the 10th Int. Particle Accelerator Conf., IPAC’19*, JACoW Publishing, Geneva, Switzerland, 2019. doi: 10.18429/JACoW-IPAC2019-TUPT089

[9] C. Pierce *et al.* “Towards High Brightness from Plasmon-Enhanced Photoemitters.” *Proceedings of the 5th North American Particle Accelerator Conference, NAPAC’22*, JACoW Publishing, Geneva, Switzerland, 2022, p. USA. doi: 10.18429/JACoW-NAPAC2022-TUYD4

[10] A. Kachwala *et al.* “Ultrafast Laser Triggered Electron Emission from Ultrananocrystalline Diamond Pyramid Tip Cathode.” *Journal of Applied Physics*, vol. 135, no. 12, AIP Publishing, 27 Mar. 2024. doi: 10.1063/5.0196457

[11] D. Novko *et al.* “Plasmonically Assisted Channels of Photoemission from Metals.” *Physical Review B*, vol. 103, no. 20, American Physical Society (APS), 3 May 2021. doi: 10.1103/physrevb.103.205401

[12] R. K. Li *et al.* “Nanometer Emittance Ultralow Charge Beams from Rf Photoinjectors.” *Physical Review Special Topics - Accelerators and Beams*, vol. 15, no. 9, American Physical Society (APS), 11 Sept. 2012. doi: 10.1103/physrevstab.15.090702

[13] Z. Guo *et al.* “Review of the Functions of Archimedes’ Spiral Metallic Nanostructures.” *Nanomaterials*, vol. 7, no. 11, MDPI AG, 22 Nov. 2017, p. 405. doi: 10.3390/nano7110405

[14] E. Ruska. “The Development of the Electron Microscope and of Electron Microscopy.” *Reviews of Modern Physics*, vol. 59, no. 3, American Physical Society (APS), 1 July 1987, pp. 627–638. doi: 10.1103/revmodphys.59.627

[15] R. J. England *et al.* “Dielectric Laser Accelerators.” *Reviews of Modern Physics*, vol. 86, no. 4, American Physical Society (APS), 23 Dec. 2014, pp. 1337–1389. doi: 10.1103/revmodphys.86.1337

[16] K. H. Siddiqui *et al.* “Relativistic Ultrafast Electron Diffraction at High Repetition Rates.” *Structural Dynamics*, vol. 10, no. 6, AIP Publishing, 1 Nov. 2023. doi: 10.1063/4.0000203

[17] Ansys-Lumerical-FDTD, <https://www.ansys.com>

[18] R. H. Fowler “The Analysis of Photoelectric Sensitivity Curves for Clean Metals at Various Temperatures.” *Physical Review*, vol. 38, no. 1, American Physical Society (APS), 1 July 1931, pp. 45–56. doi: 10.1103/physrev.38.45

[19] L. DuBridge. “A Further Experimental Test of Fowler’s Theory of Photoelectric Emission.” *Physical Review*, vol. 39, no. 1, American Physical Society (APS), 1 Jan. 1932, pp. 108–118. doi: 10.1103/physrev.39.108

[20] A. Kachwala *et al.* “Study of nano-structured electron sources using photoemission electron microscope”, in *Proc. IPAC’23*, Venice, Italy, May 2023, pp. 2174–2177. doi: 10.18429/JACoW-IPAC2023-TUPL188

[21] FOCUS-IS-IEF-PEEM, <https://www.focus-gmbh.com/peem-nanoesca/peem/>

[22] R. Bormann *et al.* “Tip-Enhanced Strong-Field Photoemission.” *Physical Review Letters*, vol. 105, no. 14, American Physical Society (APS), 27 Sept. 2010. doi: 10.1103/physrevlett.105.147601

[23] A. Kachwala *et al.* “Quantum Efficiency, Photoemission Energy Spectra, and Mean Transverse Energy of Ultrananocrystalline Diamond Photocathode.” *Journal of Applied Physics*, vol. 132, no. 22, AIP Publishing, 9 Dec. 2022. doi: 10.1063/5.0130114

[24] P. Saha *et al.* “Theory of Photoemission from Cathodes with Disordered Surfaces.” *Journal of Applied Physics*, vol. 133, no. 5, AIP Publishing, 6 Feb. 2023. doi: 10.1063/5.0135629

[25] C. Tusche *et al.* “Spin Resolved Bandstructure Imaging with a High Resolution Momentum Microscope.” *Ultramicroscopy*, vol. 159, Elsevier BV, Dec. 2015, pp. 520–529. doi: 10.1016/j.ultramic.2015.03.020

[26] M. T. Hassan. “Electron Imaging in Action: Attosecond Electron Diffraction and Microscopy.” *Structural Dynamics with X-Ray and Electron Scattering*, Royal Society of Chemistry, 20 Dec. 2023, pp. 535–556. doi: 10.1039/bk9781837671564-00535